

# Low-Frequency Noise in Ambipolar Carbon Nanotube Transistors

Ju Hee Back,<sup>†</sup> Sunkook Kim,<sup>‡</sup> Saeed Mohammadi,<sup>‡</sup> and Moonsub Shim<sup>\*†</sup>

*Department of Materials Science and Engineering, University of Illinois at Urbana–Champaign, Urbana, Illinois 61801, and School of Electrical and Computer Engineering and Birck Nanotechnology Center, Purdue University, West Lafayette, Indiana 47907*

Received December 1, 2007; Revised Manuscript Received February 3, 2008

## ABSTRACT

Low-frequency noise measurements on individual single-walled carbon nanotube transistors exhibiting ambipolar characteristics have been carried out. With a polymer electrolyte as gate medium, low-frequency noise can be monitored in both p- and n-channel operation of the same nanotube under the same chemical environment.  $1/f$  noise in the p-channel of polymer electrolyte gated nanotube transistor is similar to that of back gate operation. However, most devices exhibit significantly larger noise amplitude in the n-channel operation that has a distinct dependence on the threshold voltage. A nonuniform energy distribution of carrier trapping/scattering sites is considered to explain these observations.

Numerous interesting phenomena in one dimension have been and continue to be observed in single-walled carbon nanotubes (SWNTs).<sup>1</sup> In addition, a combination of excellent electrical and mechanical properties<sup>2</sup> may provide an accessible route to advancing nascent areas such as nanoelectronics and nanoelectromechanical systems.<sup>3</sup> One potential concern in the scale-down of devices is the increasing electronic noise with decreasing size.<sup>4</sup> In carbon nanotubes,  $1/f$  noise is the predominant low-frequency fluctuation and noise power spectra of carbon nanotubes have been reported in different device geometries.<sup>5,6</sup> Initial studies have focused primarily on three-dimensional (3D) mats and two-dimensional (2D) networks and have shown a pronounced  $1/f$  noise that scales with device resistance and channel length.<sup>5</sup> However, the complexity of these systems including contributions from tube–tube junctions, distribution of chiralities, and difficulties in determining carrier density has made it difficult to interpret  $1/f$  noise measurements. Hence, there is an increasing interest in  $1/f$  noise in devices consisting of only one SWNT. Recent studies on single tube devices have revealed that  $1/f$  noise amplitude scales inversely with the total number of carriers and, interestingly, Hooge's parameter that describes  $1/f$  fluctuations has been shown to be comparable to that of bulk semiconductors.<sup>6</sup> It has also been shown that  $1/f$  noise is independent of contact metal, and a possible source of noise has been suggested to be carrier trapping/scattering sites in the immediate surroundings of oxide

substrate<sup>6e,f</sup> or adsorbates on SWNTs.<sup>6g</sup> A notable decrease in the noise amplitude upon passivation with atomic layer deposition of  $\text{Al}_2\text{O}_3$  appears consistent with these suggestions.<sup>6d</sup>

Nearly all studies to date on  $1/f$  fluctuations in carbon nanotubes have focused on p-channel operation, i.e., on hole transport. Understanding fluctuations in electron transport is just as important not only in developing complementary devices but also in elucidating the source of  $1/f$  noise. In 2D random percolating network devices, the increasing  $1/f$  noise near the inversion point (from p- to n-channel operation) has been suggested to arise from an enhanced susceptibility to fluctuations due to increasing nonuniformity of the conduction paths.<sup>5b</sup> In addition to this nonuniformity effect, the complexity of 2D random networks and the limited n-channel operation achievable make it difficult to observe possible differences between noise characteristics of p- and n-channels. In single tube devices, there is only one report of  $1/f$  noise in an n-type device achieved by alkali metal doping.<sup>6a</sup> In this case, direct comparison may be complicated by the altered chemical environment.

Polymer electrolyte gating provides a unique opportunity to compare low-frequency noise in hole and electron transport regimes of the same SWNT under the same chemical environment. We have previously shown that varying the electron withdrawing/donating ability of the surrounding polymers can tune the operation regime from p-type to ambipolar to n-type.<sup>7</sup> Electrochemical gating provides large double layer capacitance which leads to overall gate capacitance dominated by the quantum capacitance of

\* Corresponding author: mshim@uiuc.edu.

<sup>†</sup> University of Illinois at Urbana–Champaign.

<sup>‡</sup> Purdue University.

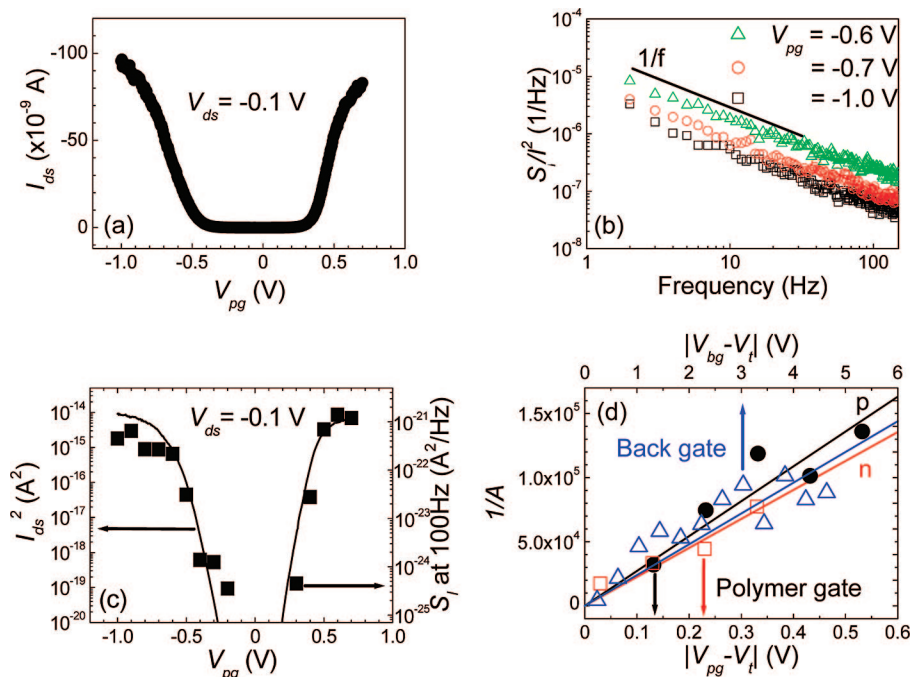


**Figure 1.** (a) Transfer characteristics of a PEG-based polymer electrolyte gated SWNT transistor at drain–source bias  $V_{ds} = -0.1$  V. (b) Normalized current noise power spectra at the indicated polymer gate voltages  $V_{pg}$ . (c) Gate dependence of  $I_{ds}^2$  (solid line) and of the current noise power at 100 Hz (squares). (d) Comparison of inverse noise amplitude of the same SWNT operated with back gate (triangles) and with polymer electrolyte gate (circles for p-channel and squares for n-channel). Lines are linear fits.

the SWNT rather than the geometric capacitance.<sup>8</sup> It has additional advantages of nearly ideal gate efficiencies and an essential elimination of hysteresis which is commonly observed in back-gating with heavily doped Si substrates.<sup>7</sup> The latter advantage is particularly important in that hysteresis will complicate quantifying the total number of carriers present—a critical value for understanding  $1/f$  noise behavior. Here, we present low-frequency noise characteristics of individual ambipolar SWNT transistors. We first show that the noise amplitude of p-channel operation is comparable to that measured for back-gate operation. We then examine  $1/f$  noise in the n-channel operation where the variations in the noise amplitude depend on the threshold voltage of the device.

SWNTs were grown by chemical vapor deposition utilizing patterned  $\text{Fe}(\text{NO}_3)_3 \cdot 9\text{H}_2\text{O}$  and alumina catalysts with  $\text{CH}_4$  and  $\text{H}_2$ .<sup>9</sup> SWNT transistors were fabricated on Si substrates with 350 nm thermal oxide. Au (35 nm with 5 nm Ti wetting layer) electrodes with 4  $\mu\text{m}$  channel length were patterned for electrical contacts. Polymer electrolytes consist of 15:1 weight ratio of the host polymer and  $\text{LiClO}_4 \cdot 3\text{H}_2\text{O}$ . For all devices examined here, poly(ethylene glycol) methyl ether (PEG, average molecular weight = 550, Acros Organics) was used as the host polymer. Where indicated, polyethylenimine (PEI, average molecular weight = 600, Aldrich) was also examined after measurement with PEG-based polymer electrolyte. Liquid PEG-based electrolyte was injected into a poly(dimethylsiloxane) fluidic channel placed on the top of the SWNT transistor channels, and the gate potential was applied with a silver wire. PEI-based electrolyte was spin coated. Low-frequency current noise spectra were obtained with a Stanford Research Systems SR 570 amplifier and a

HP 3561A dynamic signal analyzer similar to ref 6d. All measurements were carried out at room temperature under ambient conditions.

Figure 1a shows the transfer characteristics of a SWNT transistor operated with a PEG-based polymer electrolyte gate. Ambipolar behavior is observed with equally large n-channel on-current at positive polymer electrolyte gate potentials ( $V_{pg}$ ) as that of the p-channel at negative  $V_{pg}$ . The normalized current noise power spectra,  $S_I/I_{ds}^2$  vs  $f$ , of this SWNT transistor at various  $V_{pg}$  for p-channel operation are shown in Figure 1b. Similar to previously reported p-type individual SWNT devices,<sup>6</sup> the noise power in both back-gate and polymer electrolyte gate operation can be described by Hooge’s empirical model<sup>4</sup>

$$\frac{S_I}{I_{ds}^2} = \frac{A}{f^\beta} \quad (1)$$

Here,  $I_{ds}$  is the drain–source current and  $f$  is the frequency.  $A$  is the noise amplitude given by

$$A = \frac{\alpha_H}{N} \quad (2)$$

where  $\alpha_H$  is the Hooge’s parameter and  $N$  is the total number of carriers. The normalized current noise power spectra in Figure 1b vary as  $1/f^\beta$ , where  $\beta \sim 1$ . Note that the value of  $\beta$  can deviate from 1, and this deviation is discussed further when we consider  $1/f$  noise in the n-channel. Figure 1c shows the strong correlation between the gate dependence of the noise power  $S_I$  and that of  $I_{ds}^2$  operating with polymer electrolyte gate as expected from eq 1.

Figure 1d compares the inverse noise amplitude  $1/A$  as a function of gate voltage for the same device operating under

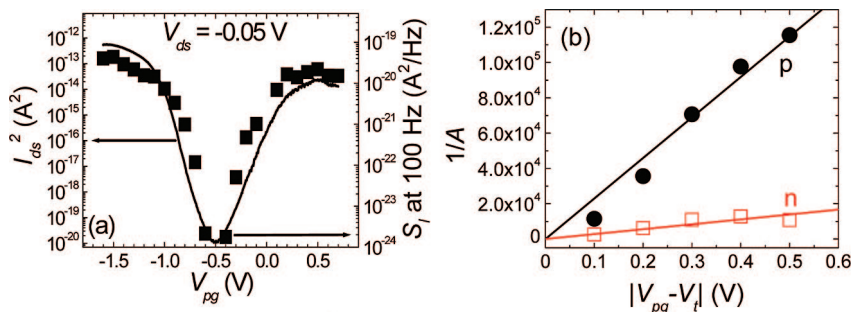


**Figure 2.** (a) Gate dependence of  $I_{ds}^2$  (solid line) and of the current noise power  $S_1$  at 100 Hz (squares) for another single SWNT device. (b) Comparison of the inverse noise amplitude  $1/A$  of p- and n-channels.

back-gate and polymer electrolyte gate. In order to quantify the gate dependence of  $A$ , we estimate the total number of carriers as  $N \approx CV_g - V_t L/e$ , where  $C$  is the total gate capacitance,  $V_g$  is the applied gate bias,  $V_t$  is the threshold voltage,  $L$  is the channel length, and  $e$  is the electric charge. For polymer electrolyte gating, the quantum capacitance of the SWNT ( $C_Q \sim 10^{-10}$  F/m) dominates  $C$  whereas the geometric capacitance (estimated as  $C_{bg} \approx 2\pi\epsilon_0 \epsilon/\ln(2t/d) \sim 10^{-11}$  F/m, where  $\epsilon_0$  is the permittivity of free space,  $\epsilon$  and  $t$  are the dielectric constant and the thickness of the  $\text{SiO}_2$  gate dielectric, respectively, and  $d$  is the diameter of the SWNT) dominates in the back-gate operation. With these values for the capacitances, the inverse noise amplitude is fitted with eq 2 resulting in  $\alpha_H = 0.009$  for p-channel polymer electrolyte gating and 0.01 for back-gating. Seven other devices examined here exhibit  $\alpha_H$  values of 0.006, 0.01, 0.011, 0.013, 0.014, 0.021, and 0.18 for p-channel operation under PEG-based polymer electrolyte gate. With the exception of the last device, these values are very similar to the reported values<sup>6</sup> for back-gating suggesting that the surrounding polymer electrolyte does not cause additional noise to the system. An order of magnitude larger value of the last device is discussed below with  $1/f$  noise in the n-channel.

Figure 1d also compares the inverse noise amplitude  $1/A$  vs  $|V_{pg} - V_t|$  of p- and n-channels for the same device. Both p- and n-channels show linear dependence with  $|V_{pg} - V_t|$  as shown by the fit. Similar slopes of  $1/A$  for the n-channel leads to similar  $\alpha_H$  value of 0.011 for this nanotube. However, other ambipolar devices show 1 to 2 orders of magnitude larger  $\alpha_H$  for the n-channel operation than that for the p-channel. Figure 2a compares the gate dependence of  $I_{ds}^2$  with that of the current noise power  $S_1$  of another single tube device. Much like the device in Figure 1,  $1/f$  noise of this SWNT transistor can be described well following Hooge's empirical model. However, unlike the device in Figure 1, the noise amplitude is significantly larger in the n-channel operation as shown by the order of magnitude difference in the slopes of  $1/A$  in Figure 2b. This difference leads to an order of magnitude larger  $\alpha_H$  for the n-channel ( $\alpha_H = 0.011$  for p-channel and 0.16 for n-channel).

In order to compare  $1/f$  noise characteristics of different devices measured, we plot  $\alpha_H$  as a function of the device threshold voltage for eight different single tube devices in Figure 3. Each color corresponds to one SWNT with p-channel values represented by filled circles and the

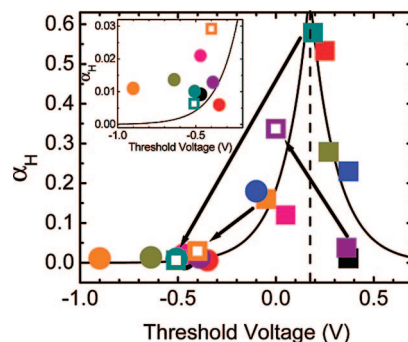


**Figure 3.** Hooge's parameter  $\alpha_H$  plotted as a function of threshold voltage for eight different single SWNT devices. Each color corresponds to one SWNT device. Filled circles are  $\alpha_H$  values for p-channel and filled squares for n-channel measured under PEG electrolyte. Open squares are n-channel  $\alpha_H$  values for PEI-gating. The curve is an exponential fit as described in the text. Each arrow corresponds to one device and indicates the change in the n-channel threshold voltage and  $\alpha_H$  upon changing the host polymer from PEG to PEI. Inset is the same data scaled to show the low  $\alpha_H$  values at negative voltages.

n-channel by filled squares. In semiconductor devices, it is well-known that sample preparation can be an important factor in the noise amplitude that devices exhibit.<sup>10</sup> Here all SWNT devices have been fabricated in the same manner and the device-to-device variation arising from sample preparation is not likely to explain the 2 orders of magnitude spread in  $\alpha_H$ . In fact, the same device with the same nanotube operating with exactly the same polymer electrolyte gate medium exhibits 2 orders of magnitude larger  $\alpha_H$  value for the n-channel ( $\alpha_H = 0.53$ ) than the p-channel ( $\alpha_H = 0.006$ ). Furthermore, there appears to be a distinct trend in the distribution of  $\alpha_H$  with respect to  $V_t$  (i.e., a maximum near  $V_t \sim 0.2$  V and decreasing away from this value).

Since the SWNTs are in an electrochemical environment, we first need to consider potential contributions from the surrounding electrolyte solution in explaining the observed trend. The fact that  $1/f$  noise in the p-channel shows negligible difference between electrolyte gate and back-gate operations suggests that electrochemical environment may not be an important factor here. However, there is still a possibility that the electrochemical environment selectively affects the  $1/f$  noise in the n-channel. Such a situation might arise if there were redox processes at positive gate voltages near the n-channel threshold voltage or if the anions and the cations had different affinities for the SWNT. For the redox

process to explain the observed trend, it must occur around 0.2 V where the largest increase in  $\alpha_H$  is observed. At this small voltage of  $\sim 0.2$  V and, in fact, for the entire gate voltage range, there is no oxidation/reduction of the dissolved electrolyte in the polymer solution and therefore we do not anticipate solution redox processes to be a possible noise source. As for the differences between cations and anions, small  $\text{Li}^+$  ions may interact more strongly with the SWNT. In this scenario, we would expect larger noise amplitude with increasing positive gate voltages for the n-channel operation. While the increase at  $V_t \sim 0$  to 0.2 V may be consistent with this asymmetric electrostatic interaction with the electrolytes, this is not likely to account for the decreasing  $\alpha_H$  with increasing  $V_t$  at  $V_t > 0.2$  V as shown in Figure 3.

Then to explain the observed trend in  $\alpha_H$ , we consider an energy distribution of traps/scattering sites (e.g., in the oxide substrate immediately surrounding the SWNT or strongly adsorbed species directly on SWNT). If the distribution of trapping/scattering sites were uniform, we would expect  $\alpha_H$  to be constant with  $V_t$ . For simplicity, we consider a distribution of trapping/scattering sites where the number of sites decays exponentially from a maximum at some fixed potential ( $V_{t/s}$ ). Then  $\alpha_H$  can be expressed as

$$\alpha_H(V) = \alpha_0 \exp\left(-\frac{|V - V_{t/s}|}{V_0}\right) \quad (3)$$

Here  $V_0$  is the spread or the distribution parameter of the exponential. The choice of an exponential distribution is from following previous works on semiconductor devices<sup>11</sup> and may be somewhat arbitrary, but the key aspect we are looking for here lies in  $V_{t/s}$  (i.e., where the majority of the trapping/scattering sites are energetically, not in the details of the functional form of the spread of such sites). The curve in Figure 3 is the fit using eq 3. Notice that most p-channel threshold voltages are sufficiently far away from  $V_{t/s}$  of  $\sim 0.2$  V such that  $\alpha_H$  is nearly constant. One device that exhibits an anomalously large  $\alpha_H$  value of 0.18 is due to the p-channel threshold voltage being closer to  $V_{t/s}$ . Since the threshold voltage is directly related to the relative band edge positions, this means that the valence band edge of this SWNT lies closer to  $V_{t/s}$  and therefore p-channel operation of this device leads to significantly larger noise levels than other devices. The n-channel threshold voltages of all devices examined here with PEG-based electrolyte gate, on the other hand, lie very close to  $V_{t/s}$  unlike most p-channel threshold voltages. The conduction band edge lying close to  $V_{t/s}$  can then explain the relatively large  $1/f$  noise. We note that when there is an energy distribution of traps/scattering sites,  $1/f$  noise can begin to deviate from the  $1/f$  dependence. That is,  $\beta$  in eq 1 can deviate from 1 ( $\beta \rightarrow 1$  as  $V_0 \rightarrow \infty$ , i.e. a uniform energy distribution of trapping/scattering sites). The n-channel operation of SWNT devices with relatively large  $\alpha_H$  values indeed exhibit this deviation with  $\beta$  as small as  $\sim 0.8$ .

To further test the idea that the threshold voltage dependent  $1/f$  noise originates from a source that lies close to the conduction band edge (under PEG-based electrolyte solu-

tion), we have examined three of the eight devices under PEI-based electrolyte where the host polymer PEI shifts the threshold voltage via electron transfer.<sup>7</sup> Under PEI gating, all three devices exhibit unipolar n-channel operation in the gate voltage range examined. The open squares in Figure 3 are the n-channel  $\alpha_H$  values for PEI-gating. The corresponding  $\alpha_H$  values from PEG gating are indicated by the arrows. The  $\alpha_H$  values for two devices decrease whereas the third device exhibits an increase. PEI adsorption causes a negative shift in the threshold voltage and a shift in the position of the conduction band edge with respect to  $V_{t/s}$ . The two SWNT devices that exhibit decreasing n-channel noise start out with their conduction band edges near  $V_{t/s}$  and therefore relatively large noise under PEG-gate. PEI adsorption causes a negative shift in the threshold voltage placing the conduction band edge away from  $V_{t/s}$  which in turn leads to a significant decrease in  $\alpha_H$  from 0.58 to 0.006 for the first device and 0.16 to 0.029 for the second device. The third device starts out with the threshold voltage more positive than  $V_{t/s}$  under PEG-electrolyte. The negative shift of the threshold voltage upon PEI adsorption also occurs for this device, but now the conduction band edge is closer to  $V_{t/s}$  leading to an order of magnitude larger noise ( $\alpha_H$  increase from 0.037 to 0.34).

Finally, we note that while this paper was under review, Mannik et al.<sup>12</sup> have reported low-frequency noise measurements on aqueous electrolyte-gated carbon nanotube transistors. Similar to our results, they find that the surrounding electrolyte solution has a negligible effect on the  $1/f$  noise of the devices.

We have presented the first low-frequency noise measurements on polymer electrolyte-gated SWNT transistors. The ability to achieve ambipolar devices has allowed us to examine how  $1/f$  noise varies for electron and hole conduction in the same nanotube under the same chemical environment. Two orders of magnitude variations in  $\alpha_H$  values can be explained by an energy distribution of traps or carrier scattering sites. Our results indicate that these sites are mostly near the conduction band edge of SWNTs under PEG-based electrolytes leading to significantly larger  $1/f$  noise in the n-channel operation.

**Acknowledgment.** This material is based upon work supported by the NSF (Grant Nos. CCF-0506660 and DMR-0348585).

## References

- (1) (a) Ilani, S.; Donev, L. A. K.; Kindermann, M.; McEuen, P. L. *Nat. Phys.* **2006**, *2*, 687. (b) Nguyen, K. T.; Gaur, A.; Shim, M. *Phys. Rev. Lett.* **2007**, *98*, 145504. (c) Kim, N. Y.; Recher, P.; Oliver, W. D.; Yamamoto, Y.; Kong, J.; Dai, H. *Phys. Rev. Lett.* **2007**, *99*, 036802.
- (2) (a) Yaish, Y.; Park, J.-Y.; Rosenblatt, S.; Sazonova, V.; Brink, M.; McEuen, P. L. *Phys. Rev. Lett.* **2004**, *92*, 046401. (b) Javey, A.; Guo, J.; Wang, Q.; Lundstrom, M.; Dai, H. *Nature* **2003**, *424*, 654. (c) Yu, M.-F.; Files, B. S.; Arepalli, S.; Ruoff, R. S. *Phys. Rev. Lett.* **2000**, *84*, 5552.
- (3) (a) Yaish, A.; Kim, H.; Brink, M.; Wang, Q.; Ural, A.; Guo, J.; McIntyre, P.; McEuen, P. L.; Lundstrom, M.; Dai, H. *Nat. Mater.* **2002**, *1*, 241. (b) Sazonova, V.; Yaish, Y.; Üstünel, H.; Roundy, D.; Arias, T. A.; McEuen, P. L. *Nature* **2004**, *431*, 284.
- (4) Hooge, F. N. *Phys. Lett.* **1969**, *29A*, 139.

- (5) (a) Collins, P. G.; Fuhrer, M. S.; Zettl, A. *Appl. Phys. Lett.* **2000**, *76*, 894. (b) Snow, E. S.; Novak, J. P.; Lay, M. D.; Perkins, F. K. *Appl. Phys. Lett.* **2004**, *85*, 4172.
- (6) (a) Lin, Y.-M.; Appenzeller, J.; Knoch, J.; Chen, Z.; Avouris, P. *Nano Lett.* **2006**, *6*, 930. (b) Ishigami, M.; Chen, J. H.; Williams, E. D.; Tobias, D.; Chen, Y. F.; Fuhrer, M. S. *Appl. Phys. Lett.* **2006**, *88*, 203116. (c) Liu, F.; Wang, K. L.; Zhang, D.; Zhou, C. *Appl. Phys. Lett.* **2006**, *89*, 063116. (d) Kim, S. K.; Xuan, Y.; Ye, P. D.; Mohammadi, S.; Back, J. H.; Shim, M. *Appl. Phys. Lett.* **2007**, *90*, 163108. (e) Lin, Y.-M.; Appenzeller, J.; Chen, Z.; Avouris, P. *Physica E* **2007**, *37*, 72. (f) Lin, Y.-M.; Tsang, J. C.; Freitag, M.; Avouris, Ph. *Nanotechnology* **2007**, *18*, 295202. (g) Tobias, D.; Ishigami, M.; Tselev, A.; Barbara, P.; Williams, E. D.; Lobb, C. J.; Fuhrer, M. S. *Phys. Rev. B* **2008**, *77*, 033407.
- (7) (a) Siddons, G. P.; Merchin, D.; Back, J. H.; Jeong, J. K.; Shim, M. *Nano Lett.* **2004**, *4*, 927. (b) Ozel, T.; Gaur, A.; Rogers, J. A.; Shim, M. *Nano Lett.* **2005**, *5*, 905. (c) Shim, M.; Ozel, T.; Gaur, A.; Wang, C. J. *J. Am. Chem. Soc.* **2006**, *128*, 7522.
- (8) (a) Back, J. H.; Shim, M. *J. Phys. Chem. B* **2006**, *110*, 23736. (b) Rosenblatt, S.; Yaish, Y.; Park, J.; Gore, J.; Sazonova, V.; McEuen, P. L. *Nano Lett.* **2002**, *2*, 869. (c) Krüger, M.; Buitelaar, M. R.; Nussbaumer, T.; Schönenberger, C.; Forró, L. *Appl. Phys. Lett.* **2001**, *78*, 1291.
- (9) (a) Kong, J.; Soh, H. T.; Cassell, A. M.; Quate, C. F.; Dai, H. *Nature* **1998**, *395*, 878. (b) Shim, M.; Siddons, G. P. *Appl. Phys. Lett.* **2003**, *83*, 3564.
- (10) Hooge, F. N. *IEEE Trans. Electron Devices* **1994**, *41*, 1926.
- (11) Lee, J. I.; Brini, J.; Chovet, A.; Dimitriadis, C. A. *Solid-State Electron.* **1999**, *43*, 2181.
- (12) Mannik, J.; Heller, I.; Janssens, A. M.; Lemay, S. G.; Dekker, C. *Nano Lett.* **2008**, *8*, 685.

NL073140G